
DISTRIBUTIONALLY ROBUST GEOMETRIC JOINT CHANCE-CONSTRAINED OPTIMIZATION: NEURODYNAMIC APPROACHES

Ange Valli^{1,*} Siham Tassouli² Abdel Lisser^{1,3}

¹Université Paris-Saclay, CNRS, CentraleSupélec, Laboratoire des signaux et systèmes

²ENAC, OPTIM

³Université Paris-Saclay, CNRS, CentraleSupélec, Fédération de Mathématiques de CentraleSupélec

{ange.valli, abdel.lisser}@l2s.centralesupelec.fr

siham.tassouli@enac.fr

March 17, 2026

ABSTRACT

This paper proposes a two-time scale neurodynamic duplex approach to solve distributionally robust geometric joint chance-constrained optimization problems. The probability distributions of the row vectors are not known in advance and belong to a certain distributional uncertainty set. In our paper, we study three uncertainty sets for the unknown distributions. The neurodynamic duplex is designed based on three projection equations. The main contribution of our work is to propose a neural network-based method to solve distributionally robust joint chance-constrained optimization problems that converges in probability to the global optimum without the use of standard state-of-the-art solving methods. We show that neural networks can be used to solve multiple instances of a problem. In the numerical experiments, we apply the proposed approach to solve a problem of shape optimisation and a telecommunication problem.

Keywords Dynamical neural network · Distributionally robust optimization · Joint chance constraints · Particle swarm optimization · Two-timescale system

1 Introduction

Chance-constrained programming appears with the increased need to include uncertainty in complex decision-making models. It was introduced for the first time by Charnes & Cooper Charnes and Cooper [1959]. Since then, chance-constrained optimization has been widely studied, and the range of applications is very large, e.g., resource allocation in communication and network systems Kandukuri and Boyd [2002], Hadi and Pakravan [2017], information theory Posada et al. [2020], chemical engineering Sonmez et al. [1999], computational finance Kabanov and Klüppelberg [2004], Zhang et al. [2012], metal cutting optimization Dupacová [2010], spatial gate sizing Singh et al. [2008], profit maximization Kojić and Lukač [2018] and biochemical systems Xu and Wang [2014], portfolio selection Han and Li [2017], energy systems operations Huo et al. [2021], water quality management Dhar and Datta [2006] and transportation problems Sluijk et al. [2023]. In this paper, we study chance-constrained geometric programs. Liu et al. Liu et al. [2016] propose some convex based approximations to come up with lower and upper bounds for geometric programs with joint probabilistic constraints when the stochastic parameters are normally distributed and pairwise independent. Shiraz et al. Khanjani Shiraz et al. [2017] use a duality algorithm to solve fuzzy chance-constrained geometric programs. Tassouli & Lisser Tassouli and Lisser [2023] propose a neurodynamic approach to solve geometric programs with joint probabilistic constraints with normally distributed coefficients and independent

*corresponding author

Websites: **Ange Valli**: <https://angevalli.github.io/>, **Siham Tassouli**: <https://optim.recherche.enac.fr/author/siham-tassouli/>, **Abdel Lisser**: <https://l2s.centralesupelec.fr/u/lisser-abdel/>

matrix row vectors. Liu et al. [2022] propose convex approximation based algorithms to solve distributionally robust geometric programs with individual and joint chance constraints.

Geometric programming is a method for solving a class of nonlinear problems. It is used to minimize functions that are in the form of posynomials subject to constraints of the same type. It was introduced for the first time by Duffin et al. [1967]. Since then geometric programming was employed to solve several optimization problems, e.g, resource allocation in communication and network systems Kandukuri and Boyd [2002], Hadi and Pakravan [2017], information theory Posada et al. [2020], Muqattash et al. [2006], chemical engineering Sonmez et al. [1999], computational finance Kabanov and Klüppelberg [2004], Zhang et al. [2012], metal cutting optimization Dupacová [2010], spatial gate sizing Singh et al. [2008], profit maximization Kojić and Lukač [2018] and biochemical systems Xu and Wang [2014].

In this paper, we are interested in solving joint chance-constrained geometric optimization problems. We study the case where the distribution of the random parameters is unknown, aka distributionally robust optimization. In fact, we may only know partial information about the statistical properties of the stochastic parameters. El Ghaoui & Lebret [1997] use second-order cone programming to solve least-squares problems where the stochastic parameters are not known but bounded. Bertsimas & Sim [2004] introduce a less conservative approach to solve linear optimization problems with uncertain data. Bertsimas & Brown [2009] propose a general scheme for designing uncertainty sets for robust optimization. Wiesemann et al. [2014] propose standardized ambiguity sets for modeling and solving distributionally robust optimization problems. Peng et al. [2021] study one density-based uncertainty set and four two-moments based uncertainty sets to solve games with distributionally robust joint chance constraints. Cheng et al. [2014] solve a distributionally robust quadratic knapsack problem. Dou & Animescu [2019] propose a new ambiguity set tailored to unimodal and seemingly symmetric distributions to deal with distributionally robust chance constraints. Li & Ke [2019] approximate a distributionally robust chance constraint by the worst-case Conditional Value-at-Risk. Hanasusanto et al. [2016] approximate two-stage distributionally robust programs with binary recourse decisions. Georghiou et al. [2020] propose a primal-dual lifting scheme for the solution of two-stage robust optimization problems. Xia et al. [2023a] propose an efficient solution approach to the Nash equilibrium of the distributionally robust chance-constrained games. Yang & Li [2023] use Sinkhorn ambiguity set to solve distributionally robust chance-constrained optimization problems.

Recent papers have considered the use of distributionally robust approaches in transportation network optimization problems Dai and Yang [2020], multistage distribution system planning Zare et al. [2018], portfolio optimization problems Fonseca et al. [2012], Wang et al. [2023], planning and scheduling Shang and You [2018], risk measures Postek et al. [2016], multimodal demand problems Hanasusanto et al. [2015], design of hub location Zhao et al. [2023], studying flexibility of networks Rayati et al. [2022], appointment scheduling Zhang et al. [2017], vehicle routing problems Ghosal and Wiesemann [2020] and energy and reserve dispatch Ordoudis et al. [2021].

The use of neural networks to solve optimization problems has been actively studied since the 1980s when the idea was first introduced by Tank & Hopfield [1986]. Xia & Wang [2004] present a recurrent neural network for solving nonlinear convex programming problems subject to nonlinear inequality constraints. Wang [1994] proposes a deterministic annealing neural network for convex programming. Nazemi & Omedi [2013] presents a neural network model for solving the shortest path problems. Tassouli & Lissner [2023] propose a recurrent neural network to solve geometric joint chance-constrained optimization problems. Wu & Lissner [2023] proposes a physics-informed neural network to solve multiple linear programs formulated as initial value problems. Flexible architectures of neural networks have been developed to overcome the limitations of standard feed-forward neural networks and vanilla recurrent neural networks: physics-informed neural networks (PINNs) Raissi et al. [2019], conditional recurrent neural networks (RNNs), long short-term memories (LSTMs), gated recurrent units (GRUs) Lauria and Saleh [2024]. Conditional recurrent neural networks were developed for computer vision applications Karpathy and Fei-Fei [2015], Vinyals et al. [2015]. Recently, they found applications in neuroscience Driscoll et al. [2024], optics Lauria and Saleh [2024] and big data Fan et al. [2025], allowing to incorporate external features independent in time, which condition the sequential data learned by the model.

In addition to the significant accomplishments achieved by individual recurrent neural networks, it is important to note that one-time-scale RNNs have limitations when it comes to constrained global optimization problems and more general problem domains. The dynamic behaviors of one-time-scale RNNs can exhibit drastic changes and become unpredictable when dealing with certain optimization problems. Neuroscience studies have provided evidence of the existence of two-time-scales in the brain, where different processes operate at different time scales Spitmaam et al. [2020]. Therefore, a neurodynamic model with two-time-scales is considered more biologically plausible for emulating brain functions than a model with only one-time-scale. Xia et al. [2023b] prove that two-timescale RNNs

converge faster than the one-timescale RNNs. This paper proposes a two-timescale duplex neurodynamic approach for distributionally robust joint chance-constrained optimization problems, which is formulated using a biconvex reformulation. Unlike other existing methods that give lower or upper bounds to this kind of problems, the proposed approach employs two recurrent neural networks that operate collaboratively at two different timescales and converge almost surely to a global optimal solution of the given distributionally robust optimization problem.

In this paper, we rely on the deterministic reformulations proposed in Liu et al. [2022] and propose two-timescale neural network-based solutions without using any convex approximations or relaxations. We also rely on the one-time scale neural network proposed in Tassouli and Lissner [2023] to create our two-time scale neural network.

The main contributions of our work are threefold.

- (i) On the formulation side, we reformulate two neurodynamic approaches to solve the equivalent deterministic problems of the initial robust programs.
- (ii) On the theoretical side, we show that the proposed neurodynamic approaches are stable and convergent.
- (iii) On the numerical side, we show that the proposed neurodynamic methods cover well the risk area induced by the distributionally robust chance constraints.

The rest of the paper is organized as follows. In Section 2, we study two uncertainty sets to solve a distributionally robust geometric chance-constrained optimization problem and give four deterministic equivalent problems. In Section 3, we propose a recurrent neural network to solve the first three resulting problems and prove its convergence and stability. We consider in Section 4 a duplex of two two-timescale recurrent neural networks to solve the last deterministic problem and prove its convergence almost surely to the global optimum. In Section 5, we evaluate the performances of the proposed neurodynamic approaches by solving a shape optimization problem and a telecommunication problem.

2 Problem statement and reformulation

The mathematical reformulations of the robust problems considered in this section are inspired from Liu et al. [2022], however, our theoretical results and algorithms are completely different.

A general form of a geometric program is given as follows

$$\begin{aligned} \min_{t \in \mathbb{R}_{++}^M} \quad & \sum_{i=1}^{I_0} c_i^0 \prod_{j=1}^M t_j^{a_{ij}^0}, \\ \text{s.t} \quad & \sum_{i=1}^{I_k} c_i^k \prod_{j=1}^M t_j^{a_{ij}^k} \leq 1, k = 1, \dots, K, \end{aligned} \quad (1)$$

where $c_i^k, i = 1, \dots, I_k, k = 1, \dots, K$ are positive constants and the exponents $a_{ij}^k, i = 1, \dots, I_k, j = 1, \dots, M, k = 1, \dots, K$ are real constants.

In this paper, we consider the case where the coefficients c_i are not known. Consequently, we reformulate the optimization problem (1) as follows

$$\begin{aligned} \min_{t \in \mathbb{R}_{++}^M} \quad & \sup_{\mathcal{F}_0 \in \mathcal{D}_0} \mathbb{E}_{\mathcal{F}_0} \left[\sum_{i=1}^{I_0} c_i^0 \prod_{j=1}^M t_j^{a_{ij}^0} \right], \\ \text{s.t} \quad & \inf_{\mathcal{F} \in \mathcal{D}} \mathbb{P}_{\mathcal{F}} \left(\sum_{i=1}^{I_k} c_i^k \prod_{j=1}^M t_j^{a_{ij}^k} \leq 1, k = 1, \dots, K \right) \geq 1 - \epsilon, \end{aligned} \quad (JCP)$$

where \mathcal{F}_0 is the probabilistic distribution of vector $C^0 = (c_1^0, \dots, c_{I_0}^0)^T$, \mathcal{F} is the joint distribution for $C^1 = (c_1^1, \dots, c_{I_1}^1)^T, \dots, C^k = (c_1^k, \dots, c_{I_k}^k)^T$, \mathcal{D}_0 is the uncertainty set for the probability distribution \mathcal{F}_0 , \mathcal{D} is the uncertainty set for the probability distribution \mathcal{F} and $1 - \epsilon, \epsilon \in (0, 0.5]$, is the confidence parameter for the joint constraint. This paper considers the distributionally robust geometric programs (JCP) using two different sets of uncertainty. The first set focuses on uncertainties in distributions, considering both known and unknown first two order moments. The second set incorporates first-order moments along with nonnegative support constraints.

2.1 Uncertainty Sets with First Two Order Moments

We first consider that the mean vector of $C^k, k = 1, \dots, K$ lies in an ellipsoid of size $\gamma_1^k \geq 0$ with center μ_k and that the covariance matrix of $C^k, k = 1, \dots, K$ lies in a positive semidefinite cone of

center $\Sigma_k = \{\sigma_{i,j}^k, i = 1, \dots, I_k, j = 1, \dots, M\}$. We define for every $k = 1, \dots, K$, $\mathcal{D}_k^2(\mu_k, \Sigma_k) = \left\{ \mathcal{F}_k \mid \begin{array}{l} (\mathbb{E}_{\mathcal{F}_k}[C^k] - \mu_k)^T \Sigma_k^{-1} (\mathbb{E}_{\mathcal{F}_k}[C^k] - \mu_k) \leq \gamma_1^k \\ \text{COV}_{\mathcal{F}_k}(C^k) \preceq \gamma_2^k \Sigma_k \end{array} \right\}$, where \mathcal{F}_k is the probability distribution of C^k , $\gamma_2^k \geq 0$ and $\text{COV}_{\mathcal{F}_k}$ is a covariance operator under probability distribution \mathcal{F}_k of C^k .

Based on whether the row vectors C^k , $k = 1, \dots, K$ are mutually independent or dependent, we have two cases.

2.1.1 Case (JCP) with Jointly Independent Row Vectors

Assumption 1. We assume that $\mathcal{D} = \{\mathcal{F} \mid \mathcal{F} = \mathcal{F}_1 \mathcal{F}_2 \dots \mathcal{F}_K\}$, where \mathcal{F} is the joint distribution for mutually independent random vectors C^1, C^2, \dots, C^K with marginals $\mathcal{F}_1, \mathcal{F}_2, \dots, \mathcal{F}_K$.

Theorem 1. Given Assumption 1, (JCP) is equivalent to

$$\begin{aligned} \min_{t \in \mathbb{R}_{++}^M, y \in \mathbb{R}_+^K} \quad & \sum_{i=1}^{I_0} \mu_i^0 \prod_{j=1}^M t_j^{a_{ij}^0} + \sqrt{\gamma_1^0} \sqrt{\sum_{i=1}^{I_0} \sum_{l=1}^{I_0} \sigma_{i,l}^0 \prod_{j=1}^M t_j^{a_{ij}^0 + a_{lj}^0}} \\ \text{s.t} \quad & \sum_{i=1}^{I_k} \mu_i^k \prod_{j=1}^M t_j^{a_{ij}^k} + \sqrt{\gamma_1^k} \sqrt{\sum_{i=1}^{I_k} \sum_{l=1}^{I_k} \sigma_{i,l}^k \prod_{j=1}^M t_j^{a_{ij}^k + a_{lj}^k}} \\ & + \sqrt{\frac{y_k}{1-y_k}} \sqrt{\gamma_2^k} \sqrt{\sum_{i=1}^{I_k} \sum_{l=1}^{I_k} \sigma_{i,l}^k \prod_{j=1}^M t_j^{a_{ij}^k + a_{lj}^k}} \leq 1 \quad \forall k = 1, \dots, K \\ & \prod_{k=1}^K y_k \geq 1 - \epsilon, \quad 0 < y_k \leq 1 \quad \forall k = 1, \dots, K \end{aligned} \tag{JCP}_{ind}$$

Proof. As the row vectors C^k , $k = 1, \dots, K$ are mutually independent, (JCP) is written equivalently by introducing K nonnegative auxiliary variables y_k as Tassouli and Lisser [2023].

$$\begin{aligned} \min_{t \in \mathbb{R}_{++}^M} \sup_{\mathcal{F}_0 \in \mathcal{D}_0} \quad & \mathbb{E}_{\mathcal{F}_0} \left[\sum_{i=1}^{I_0} c_i^0 \prod_{j=1}^M t_j^{a_{ij}^0} \right], \\ \text{s.t} \quad & \inf_{\mathcal{F}_k \in \mathcal{D}_k} \mathbb{P}_{\mathcal{F}_k} \left(\sum_{i=1}^{I_k} c_i^k \prod_{j=1}^M t_j^{a_{ij}^k} \leq 1 \right) \geq y_k, \forall k = 1, \dots, K, \\ & \prod_{k=1}^K y_k \geq 1 - \epsilon, \quad 0 < y_k \leq 1, \quad k = 1, \dots, K. \end{aligned}$$

By Theorem 1 in Liu et al. [2022], we conclude that (JCP) is equivalent to (JCP)_{ind}. \square

Problem (JCP_{ind}) is not convex. By applying the logarithmic transformation $r_j = \log(t_j)$, $j = 1, \dots, M$ and $x_k = \log(y_k)$, $k = 1, \dots, K$, we have the following equivalent reformulation of (JCP_{ind})

$$\begin{aligned}
 \min_{r \in \mathbb{R}^M, x \in \mathbb{R}^K} & \sum_{i=1}^{I_0} \mu_i^0 \exp \left\{ \sum_{j=1}^M a_{ij}^0 r_j \right\} + \sqrt{\gamma_1^0} \sqrt{\sum_{i=1}^{I_0} \sum_{l=1}^{I_0} \sigma_{i,l}^0 \exp \left\{ \sum_{j=1}^M (a_{ij}^0 + a_{lj}^0) r_j \right\}} \\
 \text{s.t.} & \sum_{i=1}^{I_k} \mu_i^k \exp \left\{ \sum_{j=1}^M a_{ij}^k r_j \right\} + \sqrt{\gamma_1^k} \sqrt{\sum_{i=1}^{I_k} \sum_{l=1}^{I_k} \sigma_{i,l}^k \exp \left\{ \sum_{j=1}^M (a_{ij}^k + a_{lj}^k) r_j \right\}} \\
 & + \sqrt{\gamma_2^k} \sqrt{\sum_{i=1}^{I_k} \sum_{l=1}^{I_k} \sigma_{i,l}^k \exp \left\{ \sum_{j=1}^M (a_{ij}^k + a_{lj}^k) r_j + \log \left(\frac{e^{x_k}}{1 - e^{x_k}} \right) \right\}} \leq 1 \quad \forall k = 1, \dots, K \\
 & \sum_{k=1}^K x_k \geq \log(1 - \epsilon), \quad x_k \leq 0 \quad \forall k = 1, \dots, K
 \end{aligned} \tag{JCP_{ind}^{log}}$$

Theorem 2. Liu et al. [2022] If $\sigma_{i,l}^k \geq 0$ for all i, l and k , problem (JCP_{ind}^{log}) is a convex programming problem.

2.1.2 Case (JCP) with Jointly Dependent Row Vectors.

In this case, (JCP) is equivalent to Liu et al. [2022]

$$\begin{aligned}
 \min_{t \in \mathbb{R}_{++}^M, y \in \mathbb{R}_+^K} & \sum_{i=1}^{I_0} \mu_i^0 \prod_{j=1}^M t_j^{a_{ij}^0} + \sqrt{\gamma_1^0} \sqrt{\sum_{i=1}^{I_0} \sum_{l=1}^{I_0} \sigma_{i,l}^0 \prod_{j=1}^M t_j^{a_{ij}^0 + a_{lj}^0}} \\
 \text{s.t.} & \sum_{i=1}^{I_k} \mu_i^k \prod_{j=1}^M t_j^{a_{ij}^k} + \sqrt{\gamma_1^k} \sqrt{\sum_{i=1}^{I_k} \sum_{l=1}^{I_k} \sigma_{i,l}^k \prod_{j=1}^M t_j^{a_{ij}^k + a_{lj}^k}} \\
 & + \sqrt{\frac{y_k}{1 - y_k}} \sqrt{\gamma_2^k} \sqrt{\sum_{i=1}^{I_k} \sum_{l=1}^{I_k} \sigma_{i,l}^k \prod_{j=1}^M t_j^{a_{ij}^k + a_{lj}^k}} \leq 1 \quad \forall k = 1, \dots, K \\
 & \sum_{k=1}^K y_k \geq K - \epsilon, \quad 0 < y_k \leq 1 \quad \forall k = 1, \dots, K
 \end{aligned} \tag{JCP_{dep}}$$

As for the independent case, we obtain using the same logarithmic transformation the following biconvex equivalent problem for (JCP_{dep})

$$\begin{aligned}
 \min_{r \in \mathbb{R}^M, x \in \mathbb{R}^K} & \sum_{i=1}^{I_0} \mu_i^0 \exp \left\{ \sum_{j=1}^M a_{ij}^0 r_j \right\} + \sqrt{\gamma_1^0} \sqrt{\sum_{i=1}^{I_0} \sum_{l=1}^{I_0} \sigma_{i,l}^0 \exp \left\{ \sum_{j=1}^M (a_{ij}^0 + a_{lj}^0) r_j \right\}} \\
 \text{s.t.} & \sum_{i=1}^{I_k} \mu_i^k \exp \left\{ \sum_{j=1}^M a_{ij}^k r_j \right\} + \sqrt{\gamma_1^k} \sqrt{\sum_{i=1}^{I_k} \sum_{l=1}^{I_k} \sigma_{i,l}^k \exp \left\{ \sum_{j=1}^M (a_{ij}^k + a_{lj}^k) r_j \right\}} \\
 & + \sqrt{\gamma_2^k} \sqrt{\sum_{i=1}^{I_k} \sum_{l=1}^{I_k} \sigma_{i,l}^k \exp \left\{ \sum_{j=1}^M (a_{ij}^k + a_{lj}^k) r_j + \log \left(\frac{y_k}{1 - y_k} \right) \right\}} \leq 1 \quad \forall k = 1, \dots, K \\
 & \sum_{k=1}^K y_k \geq K - \epsilon \quad 0 < y_k \leq 1 \quad \forall k = 1, \dots, K
 \end{aligned} \tag{JCP_{dep}^{log}}$$

Theorem 3. Liu et al. [2022] If $\epsilon \leq 0.5$ and $\sigma_{i,l}^k \geq 0$ for all i, l and k , problem (JCP_{dep}^{log}) is a convex programming problem.

2.2 Uncertainty Sets with Known First Order Moment and Nonnegative Support

In this section, we consider uncertainty sets with nonnegative supports and known first-order moments. The uncertainty sets for (JCP) can be formulated as follows

$$\mathcal{D}_k^3(\mu_k, \Sigma_k) = \left\{ \mathcal{F}_k \mid \mathbb{E}[C^k] = \mu^k, \mathbb{P}_{\mathcal{F}_k}[C^k \geq 0] = 1 \right\} \quad \forall k = 1, \dots, K$$

where $\mu^k > 0$.

2.2.1 Case (JCP) with Jointly Independent Row Vectors.

We first consider the case when the marginal distributions in the uncertainty set are jointly independent. Using the strong duality Liu et al. [2022], (JCP) can be reformulated as follows Peng et al. [2022]

$$\begin{aligned} \min_{t \in \mathbb{R}_{++}^M, \lambda, \beta, \pi} \quad & \sum_{i=1}^{I_0} \mu_i^0 \prod_{j=1}^M t_j^{\alpha_{ij}^0} & (JCP_{NS}^{ind}) \\ \text{s.t.} \quad & \prod_{k=1}^K y_k \geq 1 - \epsilon \quad \forall y_k \in [0, 1] \quad \forall k = 1, \dots, K \\ & y_k \lambda_k^{-1} - \lambda_k^{-1} \beta_k^T \mu^k \leq 1 \quad \forall k = 1, \dots, K \\ & \beta_k \leq 0, 0 < \lambda \leq 1 \quad \forall k = 1, \dots, K \\ & \lambda_k^{-1} \pi_k \geq 1 \quad \forall k = 1, \dots, K \\ & (-\beta_k)^{-1} \pi_k \prod_{j=1}^M t_j^{\alpha_{ij}^k} \leq 1 \quad \forall i = 1, \dots, I_k \quad \forall k = 1, \dots, K \end{aligned}$$

(JCP) can be reformulated as a convex problem using a logarithmic transformation $x_j = \log(y_j)$, $t_j = \log(r_j)$, $\tilde{\lambda}_k = \log(\lambda_k)$, $\tilde{\beta}_k = \log(-\beta_k)$, $\tilde{\pi} = \log(\pi)$. Problem (JCP_{NS}^{ind}) becomes,

$$\begin{aligned} \min_{x, r, \tilde{\lambda}, \tilde{\beta}, \tilde{\pi}} \quad & \sum_{i=1}^{I_0} \mu_i^0 \exp \left\{ \sum_{j=1}^M \alpha_{ij}^0 r_j \right\} & (JCP_{NS}^{log-ind}) \\ \text{s.t.} \quad & \sum_{k=1}^K x_k \geq \log(1 - \epsilon) \quad \forall x_k \leq 0 \quad \forall k = 1, \dots, K \\ & \exp(x_k - \tilde{\lambda}_k) + \sum_{i=1}^{I_k} \exp \left\{ -\tilde{\lambda}_k + \tilde{\beta}_i^k + \log \mu_i^k \right\} \leq 1 \quad \forall k = 1, \dots, K \\ & \tilde{\lambda}_k \leq 0 \quad \forall k = 1, \dots, K \\ & \tilde{\lambda}_k \leq \tilde{\pi}_k \quad \forall k = 1, \dots, K \\ & \tilde{\pi}_k + \sum_{j=1}^M \alpha_{ij}^k r_j - \tilde{\beta}_i^k \leq 0, \quad \forall i = 1, \dots, I_k \quad \forall k = 1, \dots, K \end{aligned}$$

2.2.2 Case (JCP) with Jointly Dependent Row Vectors.

In the case where the constraints of (JCP) are jointly dependent, we have the following deterministic equivalent

$$\begin{aligned}
 & \min_{t \in \mathbb{R}_{++}^M, \lambda, \beta, \pi} \sum_{i=1}^{I_0} \mu_i^0 \prod_{j=1}^M t_j^{a_{ij}^0}, & (JCP_{NS-ind}^{log}) \\
 & \text{s.t.} \quad \sum_{k=1}^K y_k \geq K - \epsilon, \quad 0 \leq y_k \leq 1, \quad k = 1, \dots, K, \\
 & \quad y_k \lambda_k^{-1} - \lambda_k^{-1} \beta^{kT} \mu^k \leq 1, \quad k = 1, \dots, K, \\
 & \quad \beta_k \leq 0, \quad 0 < \lambda \leq 1, \quad k = 1, \dots, K, \\
 & \quad \lambda_k^{-1} \pi_k \geq 1, \quad k = 1, \dots, K, \\
 & \quad (-\beta_k)^{-1} \pi_k \prod_{j=1}^M t_j^{a_{ij}^k} \leq 1, \quad i = 1, \dots, I_k, \quad k = 1, \dots, K,
 \end{aligned}$$

We apply a log transformation to convert (JCP_{NS-ind}^{log}) into a biconvex problem. We take $t_j = \log(r_j)$, $\tilde{\lambda}_k = \log(\lambda_k)$, $\tilde{\beta}_k = \log(-\beta_k)$, $\tilde{\pi} = \log(\pi)$ and obtain

$$\begin{aligned}
 & \min_{x, r, \tilde{\lambda}, \tilde{\beta}, \tilde{\pi}} \sum_{i=1}^{I_0} \mu_i^0 \exp \left\{ \sum_{j=1}^M a_{ij}^0 r_j \right\} & (JCP_{NS-dep}^{log}) \\
 & \text{s.t.} \quad \sum_{k=1}^K y_k \geq K - \epsilon \quad \forall y_k \in [0, 1] \quad \forall k = 1, \dots, K \\
 & \quad y_k \exp(-\tilde{\lambda}_k) + \sum_{i=1}^{I_k} \exp \left\{ -\tilde{\lambda}_k + \tilde{\beta}_i^k + \log \mu_i^k \right\} \leq 1 \quad \forall k = 1, \dots, K \\
 & \quad \tilde{\lambda}_k \leq 0, \quad \forall k = 1, \dots, K \\
 & \quad \tilde{\lambda}_k \leq \tilde{\pi}_k \quad \forall k = 1, \dots, K \\
 & \quad \tilde{\pi}_k + \sum_{j=1}^M a_{ij}^k r_j - \tilde{\beta}_i^k \leq 0 \quad \forall i = 1, \dots, I_k \quad \forall k = 1, \dots, K
 \end{aligned}$$

3 A dynamical recurrent neural network for (JCP_{dep}^{log}), (JCP_{ind}^{log}) and (JCP_{NS-ind}^{log})

The proposed neural network algorithm in this section is an important extension of the one in Tassouli & Lisser [2023].

Observe that (JCP_{dep}^{log}), (JCP_{ind}^{log}) and (JCP_{NS-ind}^{log}) can be written in the following general form

$$\begin{aligned}
 & \min_z f(z), & (2) \\
 & \text{s.t.} \quad g(z) \leq 0,
 \end{aligned}$$

where f and g are two convex functions.

For (JCP_{ind}^{log}) , $z = (r, x)^T$, $f(z) = \sum_{i=1}^{I_0} \mu_i^0 \exp \left\{ \sum_{j=1}^M a_{ij}^0 r_j \right\} + \sqrt{\gamma_1^0} \sqrt{\sum_{i=1}^{I_0} \sum_{l=1}^{I_0} \sigma_{i,l}^0 \exp \left\{ \sum_{j=1}^M (a_{ij}^0 + a_{lj}^0) r_j \right\}}$ and

$$g(z) = \left(\begin{array}{c} \sum_{i=1}^{I_1} \mu_i^1 \exp \left\{ \sum_{j=1}^M a_{ij}^1 r_j \right\} + \sqrt{\gamma_1^1} \sqrt{\sum_{i=1}^{I_1} \sum_{l=1}^{I_1} \sigma_{i,l}^1 \exp \left\{ \sum_{j=1}^M (a_{ij}^1 + a_{lj}^1) r_j \right\}} \\ + \sqrt{\frac{e^{x_1}}{1-e^{x_1}}} \sqrt{\gamma_2^1} \sqrt{\sum_{i=1}^{I_1} \sum_{l=1}^{I_1} \sigma_{i,l}^1 \exp \left\{ \sum_{j=1}^M (a_{ij}^1 + a_{lj}^1) r_j \right\}} - 1 \\ \vdots \\ \sum_{i=1}^{I_K} \mu_i^K \exp \left\{ \sum_{j=1}^M a_{ij}^K r_j \right\} + \sqrt{\gamma_1^K} \sqrt{\sum_{i=1}^{I_K} \sum_{l=1}^{I_K} \sigma_{i,l}^K \exp \left\{ \sum_{j=1}^M (a_{ij}^K + a_{lj}^K) r_j \right\}} + \\ \sqrt{\frac{e^{x_K}}{1-e^{x_K}}} \sqrt{\gamma_2^K} \sqrt{\sum_{i=1}^{I_K} \sum_{l=1}^{I_K} \sigma_{i,l}^K \exp \left\{ \sum_{j=1}^M (a_{ij}^K + a_{lj}^K) r_j \right\}} - 1 \\ \log(1 - \epsilon) - \sum_{k=1}^K x_k \\ x_1 \\ \vdots \\ x_K \end{array} \right)$$

For (JCP_{dep}^{log}) , $z = (r, x)^T$, $f(z) = \sum_{i=1}^{I_0} \mu_i^0 \exp \left\{ \sum_{j=1}^M a_{ij}^0 r_j \right\} + \sqrt{\gamma_1^0} \sqrt{\sum_{i=1}^{I_0} \sum_{l=1}^{I_0} \sigma_{i,l}^0 \exp \left\{ \sum_{j=1}^M (a_{ij}^0 + a_{lj}^0) r_j \right\}}$ and

$$g(z) = \left(\begin{array}{c} \sum_{i=1}^{I_1} \mu_i^1 \exp \left\{ \sum_{j=1}^M a_{ij}^1 r_j \right\} + \sqrt{\gamma_1^1} \sqrt{\sum_{i=1}^{I_1} \sum_{l=1}^{I_1} \sigma_{i,l}^1 \exp \left\{ \sum_{j=1}^M (a_{ij}^1 + a_{lj}^1) r_j \right\}} \\ + \sqrt{\frac{e^{x_1}}{1-e^{x_1}}} \sqrt{\gamma_2^1} \sqrt{\sum_{i=1}^{I_1} \sum_{l=1}^{I_1} \sigma_{i,l}^1 \exp \left\{ \sum_{j=1}^M (a_{ij}^1 + a_{lj}^1) r_j \right\}} - 1 \\ \vdots \\ \sum_{i=1}^{I_K} \mu_i^K \exp \left\{ \sum_{j=1}^M a_{ij}^K r_j \right\} + \sqrt{\gamma_1^K} \sqrt{\sum_{i=1}^{I_K} \sum_{l=1}^{I_K} \sigma_{i,l}^K \exp \left\{ \sum_{j=1}^M (a_{ij}^K + a_{lj}^K) r_j \right\}} + \\ \sqrt{\frac{e^{x_K}}{1-e^{x_K}}} \sqrt{\gamma_2^K} \sqrt{\sum_{i=1}^{I_K} \sum_{l=1}^{I_K} \sigma_{i,l}^K \exp \left\{ \sum_{j=1}^M (a_{ij}^K + a_{lj}^K) r_j \right\}} - 1 \\ \log(K - \epsilon) - \sum_{k=1}^K x_k \\ x_1 \\ \vdots \\ x_K \end{array} \right)$$

For (JCP_{NS-ind}^{log}) , $z = (r, x, \tilde{\lambda}, \tilde{\beta}, \tilde{\pi})^T$, $f(z) = \sum_{i=1}^{I_0} \mu_i^0 \prod_{j=1}^M t_j^{a_{ij}^0}$ and

$$g(z) = \begin{pmatrix} \log(1 - \epsilon) - \sum_{k=1}^K x_k \\ x_1 \\ \vdots \\ x_K \\ \exp(x_1 - \tilde{\lambda}_1) + \sum_{i=1}^{I_1} \exp\{-\tilde{\lambda}_1 + \tilde{\beta}_i^1 + \log \mu_i^1\} - 1 \\ \vdots \\ \exp(x_K - \tilde{\lambda}_K) + \sum_{i=1}^{I_K} \exp\{-\tilde{\lambda}_K + \tilde{\beta}_i^K + \log \mu_i^K\} - 1 \\ \tilde{\lambda}_1 \\ \vdots \\ \tilde{\lambda}_1 - \tilde{\pi}_1 \\ \vdots \\ \tilde{\lambda}_K - \tilde{\pi}_K \\ \tilde{\pi}_1 + \sum_{j=1}^M a_{ij}^1 r_j - \tilde{\beta}_i^1 \leq 0, i = 1, \dots, I_1 \\ \vdots \\ \tilde{\pi}_K + \sum_{j=1}^M a_{ij}^K r_j - \tilde{\beta}_i^K \leq 0, i = 1, \dots, I_K \end{pmatrix}$$

We know that z^* is an optimal solution of (2) if and only if the following Karush–Kuhn–Tucker (KKT) conditions are satisfied.

$$\begin{aligned} \nabla f(z) + \nabla g(z)^T \gamma &= 0 \\ \gamma &\geq 0, \gamma^T g(z) = 0 \end{aligned}$$

Now, let $z(\cdot)$ and $\gamma(\cdot)$ be two time-dependent variables. The objective is to develop a continuous-time dynamical system that converges to the KKT point of the nonlinear programming problem (2). Hence, our current goal is to construct a neural network capable of converging to the KKT point of the nonlinear programming problem (2). We can outline the neural network model associated with (2) by the following nonlinear dynamical system

$$\kappa \frac{dz}{dt} = -(\nabla f(z) + \nabla g(z)^T (\gamma + g(z))_+) \quad (3)$$

$$\kappa \frac{d\gamma}{dt} = -\gamma + (\gamma + g(z))_+ \quad (4)$$

where κ is a given convergence rate and $(x)_+ = (\max(x_1, 0), \max(x_2, 0), \dots, \max(x_n, 0))$, for each $x = (x_1, x_2, \dots, x_n) \in \mathbb{R}^n$.

Lemma 1. (z^*, γ^*) is an equilibrium point of (3)-(4) if and only if z^* is an optimal solution of (2) where γ^* is the corresponding Lagrange multiplier.

Lemma 2. For any initial point $(z(t_0), \gamma(t_0))$, there exists a unique continuous solution $(z(t), \gamma(t))$ for (3)-(4).

Lemma 3. The neural network proposed in equations (3)-(4) exhibits global stability in the Lyapunov sense. Furthermore, the dynamical network globally converges to a KKT point denoted (z^*, γ^*) where z^* is the optimal solution of the problem (2).

Proof. Let $\zeta = (z, \gamma)$, we define

$$U(\zeta) = \begin{bmatrix} -(\nabla f(z) + \nabla g(z)^T (\gamma + g(z))_+) \\ -\gamma + (\gamma + g(z))_+ \end{bmatrix}$$

First, consider the following Lyapunov function

$$E(\zeta) = \|U(\zeta)\|^2 + \frac{1}{2} \|\zeta - \zeta^*\|,$$

where $\zeta^* = (z^*, \gamma^*)$ is an equilibrium point of (3)-(4).

$\frac{dE(\zeta(t))}{dt} = \frac{dU}{dt}^T U + U^T \frac{dU}{dt} + (\zeta - \zeta^*)^T \frac{d\zeta}{dt}$. Observe that $\frac{dU}{dt} = \frac{dU}{d\zeta} \times \frac{d\zeta}{dt} = \nabla U(\zeta)U(\zeta)$. Without loss of generality suppose that there exists $p \in \mathbb{N}$ such that $(\gamma + g(z))_+ = (\gamma_1 + g_1(z)), \dots, (\gamma_p + g_p(z)), 0, \dots, 0$, and we define $g^p = (g_1, \dots, g_p)$.

We have

$$\nabla U(\zeta) = \begin{bmatrix} -(\nabla^2 f(z) + \sum_{i=1}^p \nabla^2 g^p(z) (\gamma_p + g_p(z)) + \nabla g(z)^T \nabla g(z)) & -\nabla g^p(z)^T \\ \nabla g^p(z) & S_p \end{bmatrix}$$

where $S_p = \begin{bmatrix} O_{p \times p} & O_{p \times (N-p)} \\ O_{(N-p) \times p} & I_{(N-p) \times (N-p)} \end{bmatrix}$ and N is the length of vector γ .

Since f and g are convex, then the Hessian matrices $\nabla^2 f$ and $\nabla^2 g^p$ are positive semidefinite. Furthermore $\nabla g^T \nabla g$ is positive semidefinite, we conclude that ∇U is negative semidefinite.

Back to the expression of $\frac{dE(\zeta(t))}{dt}$, we have

$$\frac{dE(\zeta(t))}{dt} = \underbrace{U^T (\nabla U + \nabla U^T) U}_{\leq 0 \text{ since } \nabla U \text{ is negative semidefinite}} + \underbrace{(\zeta - \zeta^*)^T (U(\zeta) - U(\zeta^*))}_{\leq 0 \text{ by Lemma 4 in Tassouli and Lisser [2023]}} \leq 0$$

Then, the neural network (3)-(4) is globally stable in the sense of Lyapunov. Next, similarly to the proof of Theorem 5 in Tassouli and Lisser [2023], we prove that the dynamical neural network (3)-(4) is globally convergent to (z^*, γ^*) where z^* is the optimal solution of (2). \square

The advantage of a dynamical recurrent neural network to solve problems (JCP_{dep}^{log}) , (JCP_{ind}^{log}) and (JCP_{NS-ind}^{log}) is to solve multiple instances of the problems at the same time after training the neural network. To do this, we consider a conditional recurrent neural network architecture Lauria and Saleh [2024]. This variant of RNN conditions the prediction based on a given set of external parameters $\theta \in \Theta$, which are not part of the sequential data. We consider problem data as external parameters modelling different instances of the same problem.

Let $\theta \in \Theta$ with Θ a compact set of parameters. The conditional RNN associated to equations (3)-(4) is given by the following system (5)-(6)

$$\kappa \frac{dz}{dt} = -(\nabla f_\theta(z) + \nabla g_\theta(z)^T (\gamma + g_\theta(z))_+) \quad (5)$$

$$\kappa \frac{d\gamma}{dt} = -\gamma + (\gamma + g_\theta(z))_+ \quad (6)$$

To solve multiple instances of the same problem, we consider that each θ represents a different instance of the problem data Wu and Lisser [2023]. In the case of problems (JCP_{dep}^{log}) , (JCP_{ind}^{log}) and (JCP_{NS-ind}^{log}) , we have $\theta = \{(\mu_i^k, a_i^k, \epsilon) \mid \forall k \in \llbracket 0, K \rrbracket \forall i \in I_k\}$. Each θ can also represent a combination of such data. When solving one instance of optimization problem, the parameter θ is constant, and the recurrent neural network (5)-(6) degrades to (3)-(4). To illustrate this feature, we present in Figure 1 a generalized circuit implementation realizing the system (5)-(6).

4 A two-time scale neurodynamic duplex for (JCP_{NS-dep}^{log})

(JCP_{NS-dep}^{log}) can be written in the following general form

$$\begin{aligned} \min_{z, y} f(z), \\ \text{s.t. } g(z, y) \leq 0, \end{aligned} \quad (7)$$

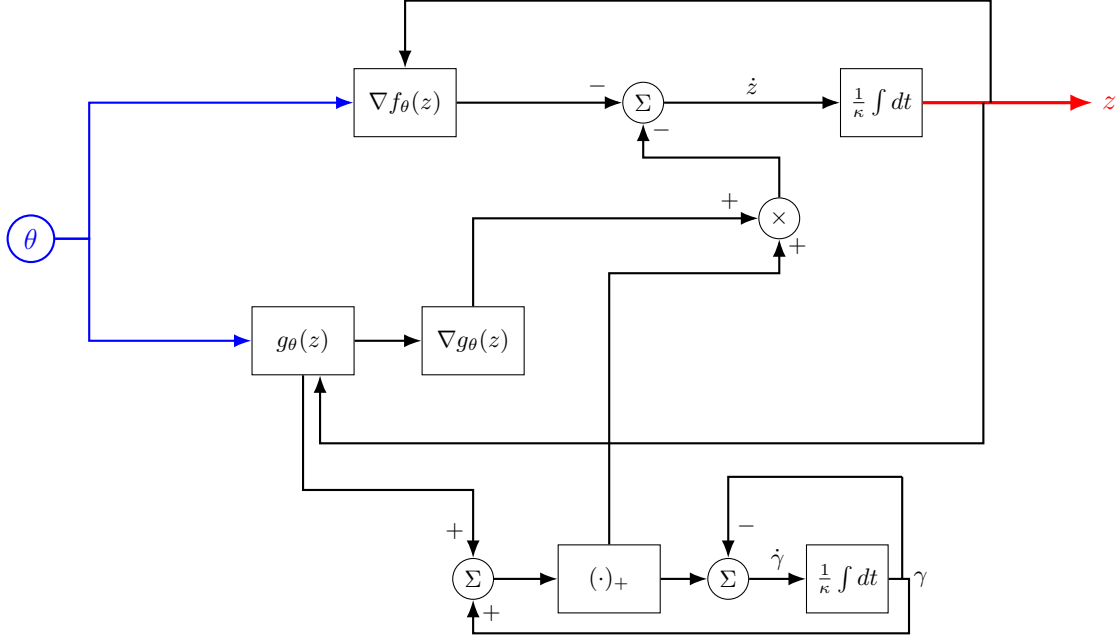


Figure 1: A block diagram for the neural network (5-6)

where f is a convex function and g is a biconvex function, $z = (r, \tilde{\lambda}, \tilde{\beta}, \tilde{\pi})^T$, $f(z) = \sum_{i=1}^{I_0} \mu_i^0 \prod_{j=1}^M t_j^{a_{ij}^0}$ and

$$g(z, y) = \begin{pmatrix} K - \epsilon - \prod_{k=1}^K y_k \\ -y_1 \\ \vdots \\ -y_K \\ y_1 - 1 \\ \vdots \\ y_K - 1 \\ y_1 \exp(-\tilde{\lambda}_1) + \sum_{i=1}^{I_1} \exp\{-\tilde{\lambda}_1 + \tilde{\beta}_i^1 + \log \mu_i^1\} - 1 \\ \vdots \\ y_K \exp(-\tilde{\lambda}_K) + \sum_{i=1}^{I_K} \exp\{-\tilde{\lambda}_K + \tilde{\beta}_i^K + \log \mu_i^K\} - 1 \\ \tilde{\lambda}_1 \\ \vdots \\ \tilde{\lambda}_1 - \tilde{\pi}_1 \\ \vdots \\ \tilde{\lambda}_K - \tilde{\pi}_K \\ \tilde{\pi}_1 + \sum_{j=1}^M a_{ij}^1 r_j - \tilde{\beta}_i^1 \leq 0, i = 1, \dots, I_1 \\ \vdots \\ \tilde{\pi}_K + \sum_{j=1}^M a_{ij}^K r_j - \tilde{\beta}_i^K \leq 0, i = 1, \dots, I_K \end{pmatrix}$$

We denote $\mathcal{U} = \{z, y \mid g(z, y) \leq 0\}$ the feasible set of (7). The Lagrangian function of problem (7) is defined as follows:

$$\mathcal{L}(z, y, \omega) = f(z) + \omega^T g(z, y). \quad (8)$$

For any $(z, y) \in \mathcal{U}$, the KKT conditions are stated as follows:

$$\nabla L(z, y, \omega) = 0, \quad (9)$$

$$\omega \geq 0, \quad \omega^T g(z, y) = 0. \quad (10)$$

Definition 1. Let $(z, y) \in \mathcal{U}$, (z, y) is called a partial optimum of (7) if and only if

$$f(z) \leq f(\tilde{z}), \forall \tilde{z} \in \mathcal{U}_y,$$

where $\mathcal{U}_y = \{z \mid g(z, y) \leq 0\}$.

Lemma 4. The KKT system (9)-(10) is equivalent to the following system

$$\nabla f(z) + \nabla_z g(z, y)^T (\omega + g(z, y))_+ = 0 \quad (11)$$

$$\nabla_y g(z, y)^T (\omega + g(z, y))_+ = 0 \quad (12)$$

$$(\omega + g(z, y))_+ - \omega = 0 \quad (13)$$

Based on the equations (11)-(13), we consider the following two-time-scale recurrent neural network model

$$\kappa_1 \frac{dz}{dt} = - (\nabla f(z) + \nabla_z g(z, y)^T (\omega + g(z, y))_+), \quad (14)$$

$$\kappa_2 \frac{dy}{dt} = - (\nabla_y g(z, y)^T (\omega + g(z, y))_+), \quad (15)$$

$$\kappa_2 \frac{d\omega}{dt} = -\omega + (\lambda + g(z, y))_+, \quad (16)$$

where (z, y, ω) are now time-dependent variables and κ_1 and κ_2 are two time scaling constants with $\kappa_1 \neq \kappa_2$. We propose a duplex of two two-time-scale recurrent neural network (14)-(16) for solving (2) one with $\kappa_1 > \kappa_2$ and the second with $\kappa_1 < \kappa_2$ as shown in Figure 2.

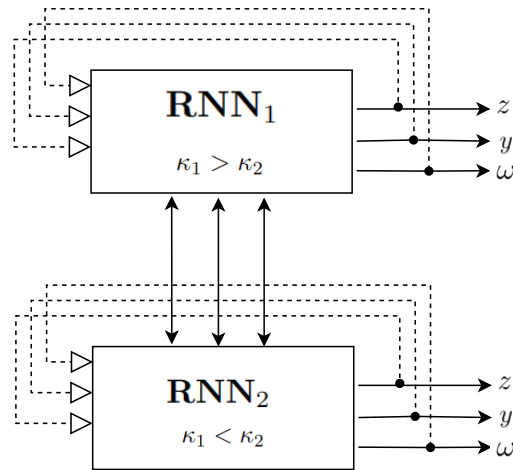


Figure 2: A block diagram depicting a duplex neurodynamic system with a two-timescale configuration

Theorem 4. (z, y, ω) is an equilibrium point of (14)-(16) if and only if (z, y, ω) is a KKT point of (7).

Proof. Let (z, y, ω) is an equilibrium point of (14)-(16). We have then

$$\begin{aligned}\frac{dz}{dt} = 0 &\iff -(\nabla f(z) + \nabla_z g(z, y)^T(\omega + g(x, z))_+) = 0 \\ \frac{dy}{dt} = 0 &\iff -(\nabla_y g(z, y)^T(\omega + g(z, y))_+) = 0 \\ \frac{d\omega}{dt} = 0 &\iff -\omega + (\lambda + g(z, y))_+ = 0.\end{aligned}$$

We obtain system (11)-(13). By Theorem 4, the conclusion follows. The converse part of the Theorem is straightforward. \square

The process begins by initializing the state variables of the neurodynamic models. Subsequently, each model undergoes a precise local search based on its dynamics to optimize its performance. Once all neurodynamic models have converged to their equilibria, the initial states of the recurrent neural networks are optimized using the particle swarm optimization (PSO) updating rule. In this context, we represent the position of the i^{th} particle as $\Lambda_i = (\Lambda_{i1}, \dots, \Lambda_{in})^T$, and its velocity as $v_i = (v_{i1}, \dots, v_{in})^T$. The inertia weight $w \in [0, 1]$ determines the extent to which the particle retains its previous velocity. The best previous position that yielded the maximum fitness value for the i^{th} particle is denoted as $\tilde{\Lambda}_i = (\tilde{\Lambda}_{i1}, \dots, \tilde{\Lambda}_{in})^T$, and the best position in the entire swarm that yielded the maximum fitness value is represented by $\hat{\Lambda} = (\hat{\Lambda}_1, \dots, \hat{\Lambda}_n)^T$. The initial state of each neurodynamic model is updated using the PSO updating rule, as described in reference Clerc and Kennedy [2002].

$$v_i(j+1) = wv_i(j) + c_1r_1(\tilde{\Lambda}_i - \Lambda_i(j)) + c_2r_2(\hat{\Lambda}_i - \Lambda_i(j)) \quad (17)$$

$$\Lambda_i(j+1) = \Lambda_i(j) + v_i(j+1). \quad (18)$$

where the iterative index is represented by j , while the two weighting parameters are denoted as c_1 and c_2 and r_1 and r_2 represent two random values from the interval $[0, 1]$.

To achieve global convergence, the diversity of initial neuronal states is crucial. One approach to enhance this diversity is by introducing a mutation operator, which generates a random $\Lambda_i(j+1)$. This random generation of $\Lambda_i(j+1)$ helps increase the variation among the initial neuronal states. To measure the diversity of these states, we employ the following function

$$d = \frac{1}{n} \sum_{i=1}^n \|\Lambda_i(j+1) - \hat{\Lambda}(j)\|.$$

We utilize the wavelet mutation operator proposed in Ling et al. [2008], which is performed for the i -th particle if $d < \zeta$. The mutation operation is carried out as follows

$$\Lambda_i(j+1) = \begin{cases} \Lambda_i(j) + \mu(h_i - \Lambda_i(j)) & \text{for } \mu > 0 \\ \Lambda_i(j) + \mu(\Lambda_i(j) - l_i) & \text{for } \mu < 0 \end{cases} \quad (19)$$

where h_i and l_i are the upper and the lower bounds for Λ_i , respectively. $\zeta > 0$ is a given threshold and μ is defined using a wavelet function

$$\mu = \frac{1}{\sqrt{a}} e^{-\frac{\phi}{2a}} \cos\left(5\frac{\phi}{a}\right) \quad (20)$$

When the value of μ goes to 1, the mutated element of the particle moves towards the maximum value of $\Lambda_i(j+1)$. On the other hand, as μ approaches -1, the mutated element moves towards the minimum value of $\Lambda_i(j+1)$. The magnitude of $|\mu|$ determines the size of the search space for $\Lambda_i(j+1)$, with larger values indicating a wider search space. Conversely, smaller values of $|\mu|$ result in a smaller search space, allowing for fine-tuning.

To achieve fine-tuning, the dilation parameter a is adjusted based on the current iteration j relative to the total number of iterations T . Specifically, a is set as a function of j/T , with $a = e^{10\frac{j}{T}}$. Additionally, ϕ is randomly generated from the interval $[-2.5a, 2.5a]$.

The algorithm details are given in Algorithm 1 where $\Lambda = (z, y, \omega)$

Lemma 5. Uryasev and Pardalos [2013] Suppose that the objective function f is measurable, and the feasible region \mathcal{U} is a measurable subset, and for any Borel subset \mathcal{B} of \mathcal{U} with positive Lebesgue measure we have $\prod_{k=1}^{\infty} (1 - \mathbb{P}_k(\mathcal{B})) = 0$.

Let $\{y(k)\}_{k=1}^{\infty}$ be a sequence generated by a stochastic optimization algorithm. If $\{y(k)\}_{k=1}^{\infty}$ is a nonincreasing sequence, then it converges in probability to the global optimum set.

Algorithm 1 The neurodynamic duplex

Initialize

- Let $\Lambda_1(0)$ and $\Lambda_2(0)$ randomly in the feasible region.
- Let the initial best previous position and best position $\tilde{\Lambda}(0) = \hat{\Lambda}(0) = y = \Lambda(0)$.
- Set the convergence error ζ .

while $\|\Lambda(j+1) - \Lambda(j)\| \geq \epsilon$ **do**

 Compute the equilibrium points $\bar{\Lambda}_1(j)$ and $\bar{\Lambda}_2(j)$ of RNN₁ and RNN₂.

if $f(\tilde{z}_1(j)) < f(\tilde{z}(j))$ **then**

$$\tilde{\Lambda}(j+1) = \bar{\Lambda}_1(j)$$

else

$$\tilde{\Lambda}(j+1) = \tilde{\Lambda}(j)$$

end if
if $f(\tilde{z}_2(j)) < f(\tilde{z}(j))$ **then**

$$\tilde{\Lambda}(j+1) = \bar{\Lambda}_2(j)$$

else

$$\tilde{\Lambda}(j+1) = \tilde{\Lambda}(j)$$

end if
if $f(\tilde{z}(j)) < f(\hat{z}(j))$ **then**

$$\hat{\Lambda}(j+1) = \tilde{\Lambda}(j+1)$$

else

$$\hat{\Lambda}(j+1) = \hat{\Lambda}(j)$$

end if

 Compute the value of $\Lambda(j+1)$ following (17)-(18).

if $d < \zeta$ **then**

Perform the wavelet mutation (19).

end if
 $j=j+1$
end while

Theorem 5. If the state of the neurodynamic model with a single timescale, described by the following equations

$$\kappa \frac{dz}{dt} = -(\nabla f(z) + \nabla_z g(z, y)^T (\omega + g(z, y)))_+ \quad (21)$$

$$\kappa \frac{dy}{dt} = -(\nabla_y g(z, y)^T (\omega + g(z, y)))_+, \quad (22)$$

$$\kappa \frac{d\omega}{dt} = -\omega + (\lambda + g(z, y))_+ \quad (23)$$

converges to an equilibrium point, then the state of the neurodynamic model with two timescales, as described by equations (14)-(16), globally converges to a partial optimum of problem (7).

Proof. We recall the Lagrangian function of (7)

$$\mathcal{L}(z, y, \omega) = f(z) + \omega^T g(z, y)$$

An equilibrium point (z^*, y^*, ω^*) of (21)-(23) corresponds to a KKT point of (7). We fix y^* , and take $z \in \mathcal{U}_{y^*}$, (7) becomes a convex optimization problem and we have

$$\mathcal{L}(z^*, y^*, \omega^*) \leq \mathcal{L}(z, y^*, \omega^*)$$

which is equivalent to

$$f(z^*) + \omega^{*T} g(z^*, y^*) \leq f(z) + \omega^{*T} g(z, y^*)$$

As $\omega^{*T} g(z, y^*) \leq \omega^{*T} g(z^*, y^*) = 0$, we have $f(z^*) \leq f(z)$. By Definition 1, (z^*, y^*) is a partial optimum of 7. \square

Theorem 6. The duplex of two two-timescale neural networks in Figure 2 is globally convergent to a global optimal solution of problem (2).

Proof. By Theorem 5, the two-timescale neurodynamic models RNN_1 and RNN_2 are proven to converge to a partial optimum. From Algorithm 1, the solution sequence is generated as follows

$$\begin{cases} \hat{\Lambda}(j+1) = \tilde{\Lambda}(j+1) & \text{if } f(\tilde{z}(j)) < f(\hat{z}(j)) \\ \hat{\Lambda}(j+1) = \hat{\Lambda}(j) & \text{otherwise} \end{cases}$$

We observe that the generated solution sequence is monotonically increasing $\{f(\hat{\Lambda}(j))\}_{j=1}^{\infty}$. Let $\mathcal{M}_{i,j}$ represent the supporting set of the initial state of RNN_i at iteration j . According to equation (19), the mutation operation ensures that the initial states of the recurrent neural networks are constrained to the feasible region \mathcal{U} . Therefore, for every iteration index $J \geq 1$, the supporting sets satisfy the following condition:

$$\mathcal{U} \subseteq \mathcal{M} = \bigcup_{j=1}^J \bigcup_{i=1}^2 \mathcal{M}_{i,j}.$$

Consequently, we have $v(\mathcal{U}) = v(\mathcal{M}) > 0$.

By Lemma 5, we have

$$\lim_{j \rightarrow \infty} \mathbb{P}(\hat{\Lambda}(j) \in \Phi) = 1$$

where Φ is the set of the global optimal solutions of (2). The conclusion follows. \square

Similarly as developed in the previous Section 3, the neurodynamic duplex allows solving multiple instances of optimization problems of the form (JCP_{NS-dep}^{log}) by considering conditional RNNs for RNN_1 and RNN_2 . Let $\theta \in \Theta$ be the parameter representing the problem data, as defined for the single recurrent neural network described by equations (3)-(4). We define the duplex of recurrent neural networks as in equations (24)-(26)

$$\kappa_1 \frac{dz}{dt} = -(\nabla f_{\theta}(z) + \nabla_z g_{\theta}(z, y)^T (\omega + g_{\theta}(x, z))_+), \quad (24)$$

$$\kappa_2 \frac{dy}{dt} = -(\nabla_y g_{\theta}(z, y)^T (\omega + g_{\theta}(z, y))_+), \quad (25)$$

$$\kappa_2 \frac{d\omega}{dt} = -\omega + (\lambda + g_{\theta}(z, y))_+, \quad (26)$$

The flowchart of the neurodynamic duplex, as described in the Algorithm 1, using conditional RNNs is presented in Figure 3.

5 Numerical experiments

We consider three geometric optimization problems to evaluate the performance of our neurodynamic approaches. All the algorithms in this Section are implemented in Python. We run our algorithms on Intel(R) Core(TM) i7-10610U CPU @ 1.80GHz. The random instances are generated with `numpy.random`, and we solve the ODE systems with `solve_ivp` of `scipy.integrate`. The deterministic equivalent programs are solved with the package GEKKO Beal et al. [2018] and the gradients and partial derivatives are computed with `autograd.grad` and `autograd.jacobian`. For the following numerical experiments, we set $\gamma_1^k = 2$, $\gamma_2^k = 2$ and the error tolerance for the neurodynamic duplex $\zeta = 10^{-4}$. In Subsection 5.2, we evaluate the quality of our neurodynamic duplex by comparing the obtained solutions with the ones given by the Convex Alternate Search (CAR) from Gorski Jochen and Kathrin [2007]. The gap between the two solutions is computed as follows $\text{GAP} = \frac{\text{Sol}_{\text{CAR}} - \text{Sol}_{\text{Duplex}}}{\text{Sol}_{\text{CAR}}}$, where Sol_{CAR} and $\text{Sol}_{\text{Duplex}}$ are the solutions obtained using the CAR and the neurodynamic duplex, respectively. For the neurodynamical duplex, we take $\frac{\kappa_1}{\kappa_2} = 0.1$ for the first dynamical neural network and $\frac{\kappa_1}{\kappa_2} = 10.0$ for the second one. We introduce conditional RNNs in the neurodynamic duplex using `cond_rnn` library https://github.com/philipperemy/cond_rnn to solve multiple instances of the problem. To evaluate the robustness of our approaches, we generate a set of 100 out-of-sample random scenarios of the stochastic constraints for each problem, and we visualize the number of scenarios for which the constraints were not respected. We call such scenarios violated scenarios (VS).

5.1 Uncertainty Sets with First Two Order Moments

5.1.1 A three-dimension shape optimization problem

We first consider a transportation problem involving the shifting of grain from a warehouse to a factory. The grain is transported within an open rectangular box, with dimensions of length x_1 meters, width x_2 meters, and height x_3

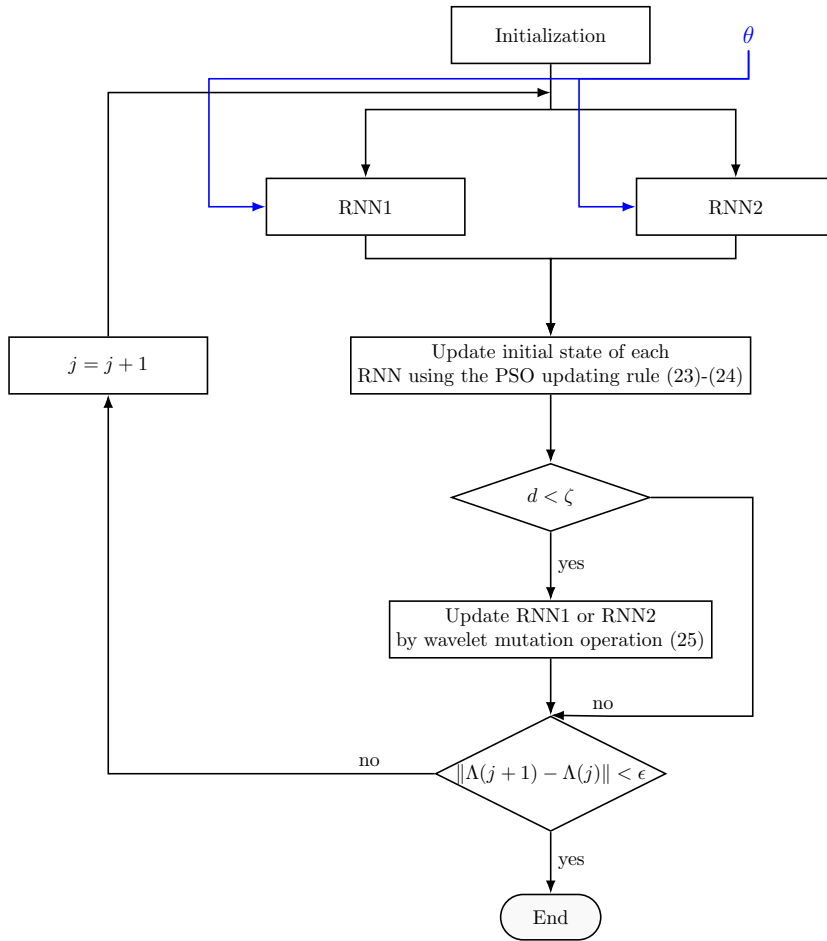


Figure 3: A block diagram of the neurodynamic duplex for the neural network (24)-(26)

meters, as illustrated in Figure 4. The objective of the problem is to maximize the volume of the rectangular box, given by the product of its length, width, and height ($x_1x_2x_3$). However, two constraints must be satisfied. The first constraint relates to the floor area of the box, and the second constraint relates to the wall area. These constraints are necessary to ensure that the shape of the box aligns with the requirements of a given truck. In our analysis, we assume that the wall area A_{wall} and the floor area A_{floor} are random variables. We formulate our shape optimization problem

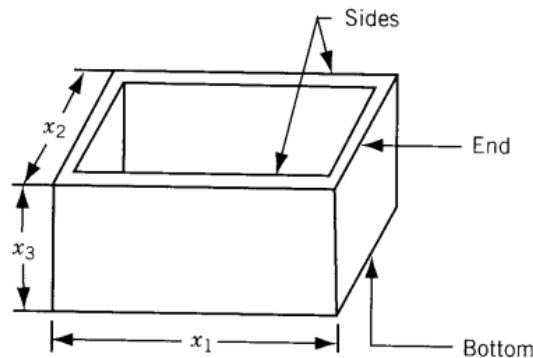


Figure 4: 3D-box shape Rao [2009]

Independent case			Dependent case		
Obj value	CPU Time	VS	Obj value	CPU Time	VS
0.296	0.43	0	0.298	0.46	0

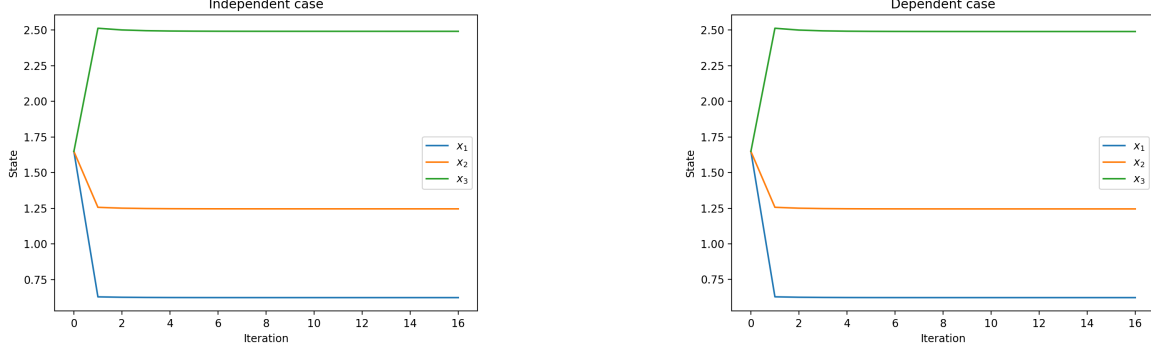
 Table 1: Results of solving problem (27) when $\mathcal{D} = \mathcal{D}^2$


Figure 5: Transient behaviors of the state variables

as follows

$$\begin{aligned}
 & \min_{x \in \mathbb{R}_{++}^3} x_1^{-1} x_2^{-1} x_3^{-1}, \\
 & \text{s.t. } \inf_{\mathcal{F} \in \mathcal{D}} \mathbb{P}_{\mathcal{F}} \left(\frac{1}{A_{wall}} (2x_3 x_2 + 2x_1 x_3) \leq 1, \frac{1}{A_{floor}} x_1 x_2 \leq 1 \right) \geq 1 - \epsilon.
 \end{aligned} \tag{27}$$

where \mathcal{F} is the joint distribution for $\frac{1}{A_{wall}}$ and $\frac{1}{A_{floor}}$ and \mathcal{D} is the uncertainty set for the probability distribution \mathcal{F} . We solve problem (27) when the uncertainty set is equal to \mathcal{D}^2 using the dynamical neural network (3)-(4). For the numerical experiments, we take the mean and the covariance describing the uncertainty sets for $\frac{1}{A_{wall}}$ $m_{wall} = 0.05$, $\sigma_{wall} = 0.01$, respectively and for $\frac{1}{A_{floor}}$ $m_{floor} = 0.5$, $\sigma_{floor} = 0.1$, respectively. We recapitulate the obtained results in Table 1. Columns 1, 2 and 3 give the optimal value, the CPU time and the number of violated scenarios (VS) in the independent case, respectively. Columns four, five and six show the optimal value, the CPU time and the number VS in the dependent case, respectively. The dynamic neural network covers well the risk region in both cases. Figure 5 show the convergence of the state variables.

5.1.2 Multidimensional shape optimization problem

To further assess the performance of our dynamical neural network, we use the multidimensional shape optimization problem with joint chance constraints from Liu et al. [2022].

$$\begin{aligned}
 & \min_{x \in \mathbb{R}_{++}^m} \prod_{i=1}^m x_i^{-1}, \\
 & \text{s.t. } \inf_{\mathcal{F} \in \mathcal{D}} \mathbb{P}_{\mathcal{F}} \left(\sum_{j=1}^{m-1} \left(\frac{m-1}{A_{wallj}} x_1 \prod_{i=1, i \neq j}^m x_i \right) \leq 1, \frac{1}{A_{floor}} \prod_{j=2}^m x_j \leq 1 \right) \geq 1 - \epsilon, \\
 & \frac{1}{\gamma_{i,j}} x_i x_j^{-1} \leq 1, 1 \leq i \neq j \leq m.
 \end{aligned} \tag{28}$$

In our numerical experiments, we fixed the following parameters $\frac{1}{\gamma_{i,j}} = 0.5$ and $\epsilon = 0.15$. The inverse of floor's area ($\frac{1}{A_{floor}}$) and the inverse of wall area ($\frac{1}{A_{wallj}}$) for each $j = 1, \dots, m$ were considered as random variables. To define the uncertainty set \mathcal{D}^2 , we generate the components of μ uniformly in $[1.0/40.0, 1.0/20.0]$ and the components of the

m	Independent case			Dependent case		
	Obj value	CPU Time	VS	Obj value	CPU Time	VS
3	1.03	1.05	4	1.30	1.39	0
5	2.09	5.11	3	2.15	5.20	1
10	14.79	4.83	2	15.10	5.04	0
15	7.76	47.80	3	7.99	58.04	1
20	10.68	97.72	2	10.87	100.91	0

Table 2: Results for different values of m

matrix Σ uniformly in $[0.001, 0.01]$. We test the robustness of the different approaches by creating 100 random samples of the variables $\frac{1}{A_{wall_j}}$ and $\frac{1}{A_{floor}}$. We then examine if the solutions meet the constraints of (28) for all 100 cases for the normal distribution. If the solutions are not feasible for a particular case, it is referred to as a violated scenario (VS).

We first solve (28) for $m = 5$ and when the uncertainty set is \mathcal{D}^2 in the independent case for different initial points, we observe that the dynamical neural network (3)-(4) converges to the same final value independently from the starting value as shown in Figure 6.

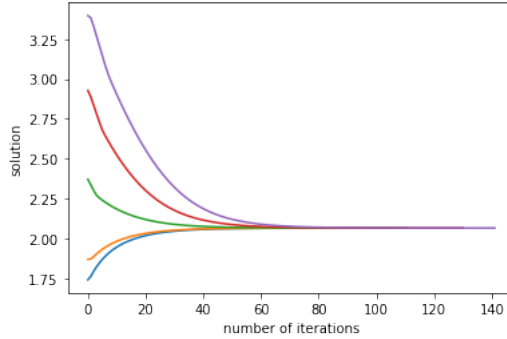


Figure 6: Convergence of the dynamical neural network (3)-(4) for different initial points for (28).

Now we solve (28) for known first-order moments of $\frac{1}{A_{floor}}$ and $\frac{1}{A_{wall_j}}$ for both the dependent and the independent case. We present the obtained results in Table 2. We observe again that the dependent case is more conservative compared to the independent one since the final values of the objective functions are lower. Nevertheless, the dependent case covers the risk area better since the number of violated scenarios is lower compared to the independent case.

5.2 Uncertainty Sets with Known First Order Moment and Nonnegative Support

5.2.1 A generalized shape optimization problem

We solve (28) when the uncertainty set is \mathcal{D}^3 for both the independent and the dependent case.

For the numerical experiments, we take $\epsilon = 0.2$. We solve problem (28) using the neurodynamic duplex in the dependent case. We recapitulate the obtained results in Table 3. Column 1 gives the number of variables m . Columns 2, 3 and 4 give the objective value, the CPU time and the number of VS, with respect to the normal distribution, in the independent case, respectively. Columns 5, 6, and 7 provide the objective value, CPU time, and the number of VS for the dependent case, respectively. We observe that the problem with dependent variables is more conservative. Nevertheless, the solution in this case covers the risk area well, as the number of VS is equal to 0 for all values of m .

Now we additionally solve problem (28) using a stochastic approach with the assumption that the random variables follow a normal distribution Tassouli and Lisser [2023] for $m = 5$. In order to compare the solutions obtained with the stochastic and the robust approaches, we evaluate the robustness of the solutions for different hypotheses on the true distribution of the random parameters, i.e., the uniform distribution, the normal distribution, the log-normal distribution, the logistic distribution and Gamma distribution. The obtained results are presented in Table 4 which gives the number of violated scenarios for both the distributed normal solutions and the robust ones and the objective value obtained by each solution. We can infer that the distributionally robust approaches are a conservative approximation

m	Independent case			Dependent case		
	Obj value	CPU Time	VS	Obj value	CPU Time	VS
3	0.204	2.28	3	0.491	10.12	0
5	1.03	6.25	2	1.82	98.68	0
10	6.99	15.26	2	9.79	86.35	0
15	18.43	23.84	3	23.45	201.13	0
20	32.09	94.76	5	38.71	744.26	0
30	42.37	100.23	3	51.56	1155.42	0

 Table 3: (28) for different values of m for $\mathcal{D} = \mathcal{D}^3$

of the stochastic programs. We observe that the solutions obtained by the nonnegative support are more conservative compared to the stochastic ones. Notice that the distributionally robust solutions are more robust, i.e., the number of VS when the true distribution is the Logistic distribution is equal to 23 and 19 for the nonnegative support solutions and is equal to 0 for the robust solutions.

		Normal solutions		Robust solutions	
		Independent	Dependent	Independent	Dependent
	Objective Value	0.86	0.99	2.43	4.14
Number of violated scenarios	Uniform distribution	22	15	0	0
	Normal distribution	18	11	1	0
	Log-normal distribution	7	4	2	1
	Logistic distribution	23	19	0	0
	Gamma distribution	16	12	2	2

Table 4: Number of violated scenarios for the stochastic and the robust solutions

5.2.2 Maximizing the worst user signal-to-interference noise ratio

We consider the problem of maximizing the worst user signal-to-interference noise ratio (SINR) for Massive Multiple Input Multiple Output (MaMIMO) systems subject to antenna assignment and multiuser interference constraints taken from Adasme and Lisser [2023] and given by

$$\max_{p \in \mathbb{R}_{++}^K} \min_{i \in \mathcal{U}} \frac{p_i |g_i^H g_i|^2}{\sum_{j \in \mathcal{U}, j \neq i} p_j |g_i^H g_j|^2 + |\sigma_i|^2}, \quad (29)$$

$$\text{s.t.} \quad P_{min} \leq p_i \leq P_{max}, \forall i \in \mathcal{U}, \quad (30)$$

where p_i is the power to be assigned for each user $i \in \mathcal{U}$. $g_i \in \mathbb{C}^{T \times 1}$, $g_i^H \in \mathbb{C}^{1 \times T}$ and σ_i^2 are the beam domain channel vector associated to user $i \in \mathcal{U}$, its Hermitian transpose and Additive White Gaussian Noise (AWGN), respectively.

Let $a_{ij} = |g_i^H g_j|^2 |g_i^H g_i|^{-2}$ and $b_i = |\sigma_i|^2 |g_i^H g_i|^{-2}$, we derive a geometric reformulation of (29)-(30)

$$\begin{aligned} & \min_{p \in \mathbb{R}_{++}^K, w \in \mathbb{R}_{++}} w^{-1} \\ & \text{s.t.} \quad \sum_{j \in \mathcal{U}, j \neq i} a_{ij} p_j p_i^{-1} w + b_i p_i^{-1} w \leq 1 \quad \forall i \in \mathcal{U} \\ & \quad \quad P_{min} \leq p_i \leq P_{max} \quad \forall i \in \mathcal{U} \end{aligned}$$

We assume that the coefficients a_{ij} and b_i are independent random variables and we propose the following optimization problem with individual and joint chance constraints

$$\begin{aligned} & \min_{p \in \mathbb{R}_{++}^K, w \in \mathbb{R}_{++}} w^{-1}, \\ & \text{s.t.} \quad \inf_{\mathcal{F}_i \in \mathcal{D}_i} \mathbb{P}_{\mathcal{F}_i} \left\{ \sum_{j \in \mathcal{U}, j \neq i} a_{ij} p_j p_i^{-1} w + b_i p_i^{-1} w \leq 1 \right\} \geq 1 - \epsilon_i, \forall i \in \mathcal{U} \quad (POI) \\ & \quad \quad P_{min} \leq p_i \leq P_{max} \quad \forall i \in \mathcal{U}. \end{aligned}$$

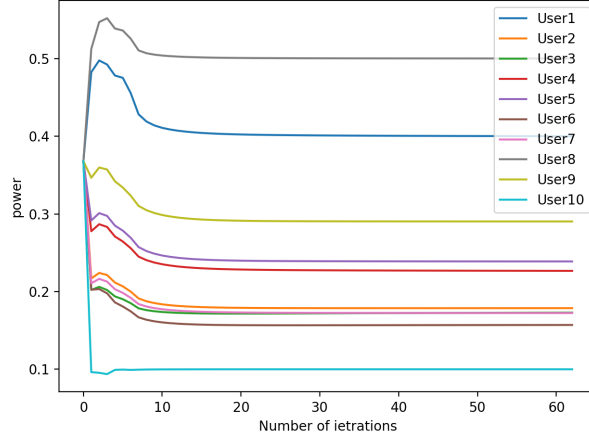


Figure 7: Convergence of the power variables

K	Individual constraints		Joint constraints	
	Obj value	VS	Obj value	VS
5	27.27	5	29.07	0
10	47.36	4	50.23	0
15	66.03	5	68.76	1
20	123.48	3	127.43	0

 Table 5: Results for different values of K

and

$$\begin{aligned}
 & \min_{p \in \mathbb{R}_{++}^K, w \in \mathbb{R}_{++}} w^{-1}, \\
 & \text{s.t.} \quad \inf_{\mathcal{F} \in \mathcal{D}} \mathbb{P}_{\mathcal{F}} \left\{ \sum_{j \in \mathcal{U}, j \neq i} a_{ij} p_j p_i^{-1} w + b_i p_i^{-1} w \leq 1, \forall i \in \mathcal{U} \right\} \geq 1 - \epsilon \quad (POJ) \\
 & \quad P_{min} \leq p_i \leq P_{max} \quad \forall i \in \mathcal{U}
 \end{aligned}$$

We assume that the uncertainty set for the distributionally robust problems (POI) and (POJ) is \mathcal{D}^3 . We fix $\epsilon = 0.2$. We first solve problem (POJ) for $K = 10$. Figure 7 shows the convergence of the power variables. Next, we solve (POI) and (POJ) for different values of the number of users K . Table 5 presents the obtained results. Column 1 gives the number of users K . Columns 2 and 3 give the optimal value and the number of VS, with respect to the normal distribution, for (POI), respectively. Columns four and five show the optimal value and the number of VS for (POJ), respectively. As observed in the previous Section 4, the use of joint constraints leads to a more conservative minimization problem but covers well the risk area compared to the problem with individual constraints since the number of VS is lower.

Now, we compare our neurodynamic duplex to the CAR method. We recapitulate the obtained results in Table 6.

For the different values of K , the GAP between both methods does not exceed 6%. Therefore, they yield similar performance results, as the differences in constraint violations and objective values are not significant. The advantage of considering the neurodynamic duplex approach over the CAR method is that it allows for obtaining solutions to multiple instances of the same problem without requiring further training. We can solve different instances of the problem by changing the parameter θ , whereas the CAR method must be applied to each instance. Once the training of the conditional recurrent neural networks RNN_1 and RNN_2 in the neurodynamic duplex has been done, the model can directly output a solution adapted to a change in the numerical values of $(a_{i,j})_{i,j \in \mathcal{U}, i \neq j}$, $(b_i)_{i \in \mathcal{U}}$ or ϵ in (POJ), represented by θ , which is a flexibility that the CAR algorithm could not offer. In Table 7, we show the computation time for multiple instances of the problem solved by both methods. We observe that our neurodynamic duplex is 100 times faster than the alternate convex search when solving 100 instances of the problem, since solving multiple

K	The neurodynamic Duplex		The Alternate Convex Search		GAP
	Obj value	VS	Obj value	VS	
5	29.03	1	31.14	4	6.77%
10	50.23	1	52.04	3	3.47%
15	66.03	0	68.66	4	3.82%
20	123.48	1	125.34	5	1.48%
30	187.55	1	189.36	4	0.95%
40	213.89	2	210.43	4	1.61%

Table 6: The neurodynamic Duplex vs. The Alternate Convex Search

Number of instances	The neurodynamic Duplex	The Alternate Convex Search
1	5.11	5.03
10	4.85	50.06
20	5.22	100.21
50	5.06	250.40
100	5.01	500.62

Table 7: Comparison of CPU times, in seconds, between the neurodynamic Duplex and the Alternate Convex Search on solving multiple instances of (POJ) .

instances takes the same CPU time as solving one, whereas the alternate convex search method must be applied again entirely for each instance.

6 Conclusion

This paper studies a distributionally robust joint-constrained geometric optimization problem for two different moments-based uncertainty sets. We propose two neurodynamic approaches to solve the resulting optimization problems. To assess the performances of the proposed approaches, we solve a problem of shape optimization and a telecommunication problem. We observe that our approach is robust since it covers well against the fluctuations of the risk area. The neurodynamic approach exhibits a key advantage in its ability to converge closer to the optimal solution, whereas the alternate convex search method only provides an upper bound due to its convex approximation. In our numerical experiments, we obtain similar results for both methods in terms of objective value and constraints violations, but the neurodynamic duplex is significantly faster than the alternate convex search in CPU times for solving multiple instances of a problem. This distinction underscores the superior accuracy and effectiveness of our approach.

We note that the performances of our approaches can be significantly increased with the development of new ODE solvers mainly based on machine learning techniques.

References

- Pablo Adasme and Abdel Lisser. A stochastic geometric programming approach for power allocation in wireless networks. *Wireless Networks*, 2023. doi: 10.1007/s11276-023-03295-8.
- Logan Beal, Daniel Hill, R Martin, and John Hedengren. Gekko optimization suite. *Processes*, 6(8):106, 2018. doi: 10.3390/pr6080106.
- Dimitris Bertsimas and David B Brown. Constructing uncertainty sets for robust linear optimization. *Operations research*, 57(6):1483–1495, 2009.
- Dimitris Bertsimas and Melvyn Sim. The price of robustness. *Operations research*, 52(1):35–53, 2004.
- Abraham Charnes and William W Cooper. Chance-constrained programming. *Management science*, 6(1):73–79, 1959.
- Jianqiang Cheng, Erick Delage, and Abdel Lisser. Distributionally robust stochastic knapsack problem. *SIAM Journal on Optimization*, 24(3):1485–1506, 2014.
- Maurice Clerc and James Kennedy. The particle swarm-explosion, stability, and convergence in a multidimensional complex space. *IEEE transactions on Evolutionary Computation*, 6(1):58–73, 2002.

- Qian Dai and Jiaqi Yang. A distributionally robust chance-constrained approach for modeling demand uncertainty in green port-hinterland transportation network optimization. *Symmetry*, 12(9):1492, 2020.
- A Dhar and B Datta. Chance constrained water quality management model for reservoir systems. *ISH Journal of Hydraulic Engineering*, 12(3):39–48, 2006.
- Xialiang Dou and Mihai Anitescu. Distributionally robust optimization with correlated data from vector autoregressive processes. *Operations Research Letters*, 47(4):294–299, 2019. ISSN 0167-6377. doi: <https://doi.org/10.1016/j.orl.2019.04.005>.
- Laura N Driscoll, Krishna Shenoy, and David Sussillo. Flexible multitask computation in recurrent networks utilizes shared dynamical motifs. *Nature Neuroscience*, 27(7):1349–1363, 2024.
- R J Duffin, E Peterson, and C Zener. *Geometric Programming*. Wiley, New York, 1967.
- J. Dupacová. Stochastic geometric programming with an application. *Kybernetika*, 46:374–386, 2010.
- Laurent El Ghaoui and Hervé Lebret. Robust solutions to least-squares problems with uncertain data. *SIAM Journal on matrix analysis and applications*, 18(4):1035–1064, 1997.
- Boyu Fan, Alex Sim, Kesheng Wu, and Jinh Kim. Conditional recurrent neural networks for enhancing throughput prediction and slow file transfers detection in large science workflows. In *2025 IEEE 22nd Consumer Communications & Networking Conference (CCNC)*, pages 1–6. IEEE, 2025.
- Raquel J Fonseca, Wolfram Wiesemann, and Berç Rustem. Robust international portfolio management. *Computational Management Science*, 9(1):31–62, 2012.
- Angelos Georghiou, Angelos Tsoukalas, and Wolfram Wiesemann. A primal–dual lifting scheme for two-stage robust optimization. *Operations Research*, 68(2):572–590, 2020.
- Shubhechyya Ghosal and Wolfram Wiesemann. The distributionally robust chance-constrained vehicle routing problem. *Operations Research*, 68(3):716–732, 2020.
- Pfeuffer Frank Gorski Jochen and Klamroth Kathrin. Biconvex sets and optimization with biconvex functions: a survey and extensions. *Mathematical Methods of Operations Research*, page 373–467, 2007. ISSN 1432-5217. doi: 10.1007/s00186-007-0161-1.
- Mohammad Hadi and Mohammad Reza Pakravan. Resource allocation for elastic optical networks using geometric optimization. *J. Opt. Commun. Netw.*, 9(10):889–899, Oct 2017. doi: 10.1364/JOCN.9.000889. URL <https://opg.optica.org/jocn/abstract.cfm?URI=jocn-9-10-889>.
- Yingwei Han and Ping Li. An empirical study of chance-constrained portfolio selection model. *Procedia Computer Science*, 122:1189–1195, 2017. ISSN 1877-0509. doi: <https://doi.org/10.1016/j.procs.2017.11.491>. URL <https://www.sciencedirect.com/science/article/pii/S1877050917327485>. 5th International Conference on Information Technology and Quantitative Management, ITQM 2017.
- Grani A Hanasusanto, Daniel Kuhn, Stein W Wallace, and Steve Zymler. Distributionally robust multi-item news vendor problems with multimodal demand distributions. *Mathematical Programming*, 152(1):1–32, 2015.
- Grani A. Hanasusanto, Daniel Kuhn, and Wolfram Wiesemann. K-adaptability in two-stage distributionally robust binary programming. *Operations Research Letters*, 44(1):6–11, 2016. ISSN 0167-6377. doi: <https://doi.org/10.1016/j.orl.2015.10.006>. URL <https://www.sciencedirect.com/science/article/pii/S0167637715001376>.
- Da Huo, Chenghong Gu, David Greenwood, Zhaoyu Wang, Pengfei Zhao, and Jianwei Li. Chance-constrained optimization for integrated local energy systems operation considering correlated wind generation. *International Journal of Electrical Power & Energy Systems*, 132:107153, 2021. ISSN 0142-0615. doi: <https://doi.org/10.1016/j.ijepes.2021.107153>. URL <https://www.sciencedirect.com/science/article/pii/S0142061521003926>.
- Yuri Kabanov and Claudia Klüppelberg. A geometric approach to portfolio optimization in models with transaction costs. *Finance and Stochastics*, 8(2):207–227, 2004.
- Sunil Kandukuri and Stephen Boyd. Optimal power control in interference-limited fading wireless channels with outage-probability specifications. *IEEE transactions on wireless communications*, 1(1):46–55, 2002.
- Andrej Karpathy and Li Fei-Fei. Deep visual-semantic alignments for generating image descriptions. In *Proceedings of the IEEE conference on computer vision and pattern recognition*, pages 3128–3137, 2015.
- Rashed Khanjani Shiraz, Madjid Tavana, Hirofumi Fukuyama, and Debora Di Caprio. Fuzzy chance-constrained geometric programming: the possibility, necessity and credibility approaches. *Operational Research*, 17(1):67–97, 2017.

- Vedran Kojić and Zrinka Lukač. Solving profit maximization problem in case of the cobb-douglas production function via weighted ag inequality and geometric programming. In 2018 IEEE International Conference on Industrial Engineering and Engineering Management (IEEM), pages 1900–1903. IEEE, 2018.
- Simone Lauria and Mohammed F Saleh. Conditional recurrent neural networks for broad applications in nonlinear optics. Optics Express, 32(4):5582–5591, 2024.
- Xiaolong Li and Jiannan Ke. Robust assortment optimization using worst-case cvar under the multinomial logit model. Operations Research Letters, 47(5):452–457, 2019. ISSN 0167-6377. doi: <https://doi.org/10.1016/j.orl.2019.07.010>. URL <https://www.sciencedirect.com/science/article/pii/S016763771830169X>.
- Sai-Ho Ling, Herbert HC Iu, Kit Yan Chan, Hak-Keung Lam, Benny CW Yeung, and Frank H Leung. Hybrid particle swarm optimization with wavelet mutation and its industrial applications. IEEE Transactions on Systems, Man, and Cybernetics, Part B (Cybernetics), 38(3):743–763, 2008.
- Jia Liu, Abdel Lisser, and Zhiping Chen. Stochastic geometric optimization with joint probabilistic constraints. Operations Research Letters, 44(5):687–691, 2016. ISSN 0167-6377. doi: <https://doi.org/10.1016/j.orl.2016.08.002>. URL <https://www.sciencedirect.com/science/article/pii/S0167637716300761>.
- Jia Liu, Abdel Lisser, and Zhiping Chen. Distributionally robust chance constrained geometric optimization. Mathematics of Operations Research, 47(4):2950–2988, 2022.
- Alaa Muqattash, Marwan Krunz, and Tao Shu. Performance enhancement of adaptive orthogonal modulation in wireless cdma systems. IEEE Journal on Selected Areas in Communications, 24(3):565–578, 2006.
- Alireza Nazemi and Farahnaz Omid. An efficient dynamic model for solving the shortest path problem. Transportation Research Part C: Emerging Technologies, 26:1–19, 2013. ISSN 0968-090X. doi: <https://doi.org/10.1016/j.trc.2012.07.005>. URL <https://www.sciencedirect.com/science/article/pii/S0968090X12000964>.
- Christos Ordoudis, Viet Anh Nguyen, Daniel Kuhn, and Pierre Pinson. Energy and reserve dispatch with distributionally robust joint chance constraints. Operations Research Letters, 49(3):291–299, 2021. ISSN 0167-6377. doi: <https://doi.org/10.1016/j.orl.2021.01.012>. URL <https://www.sciencedirect.com/science/article/pii/S0167637721000213>.
- Shen Peng, Abdel Lisser, Vikas Vikram Singh, Nalin Gupta, and Eshan Balachandar. Games with distributionally robust joint chance constraints. Optimization Letters, 15(6):1931–1953, 2021.
- Shen Peng, Francesca Maggioni, and Abdel Lisser. Bounds for probabilistic programming with application to a blend planning problem. European Journal of Operational Research, 297(3):964–976, 2022.
- Jose Gallego Posada, Ankit Vani, Max Schwarzer, and Simon Lacoste-Julien. Gait: A geometric approach to information theory. In International Conference on Artificial Intelligence and Statistics, pages 2601–2611. PMLR, 2020.
- Krzysztof Postek, Dick den Hertog, and Bertrand Melenberg. Computationally tractable counterparts of distributionally robust constraints on risk measures. SIAM Review, 58(4):603–650, 2016.
- Maziar Raissi, Paris Perdikaris, and George E Karniadakis. Physics-informed neural networks: A deep learning framework for solving forward and inverse problems involving nonlinear partial differential equations. Journal of Computational physics, 378:686–707, 2019.
- SS Rao. Geometric programming. Engineering Optimization; John Wiley & Sons, Ltd.: Hoboken, NJ, USA, pages 492–543, 2009.
- Mohammad Rayati, Mokhtar Bozorg, Rachid Cherkaoui, and Mauro Carpita. Distributionally robust chance constrained optimization for providing flexibility in an active distribution network. IEEE Transactions on Smart Grid, 13(4):2920–2934, 2022.
- Chao Shang and Fengqi You. Distributionally robust optimization for planning and scheduling under uncertainty. Computers & Chemical Engineering, 110:53–68, 2018. ISSN 0098-1354. doi: <https://doi.org/10.1016/j.compchemeng.2017.12.002>. URL <https://www.sciencedirect.com/science/article/pii/S009813541730426X>.
- Jaskirat Singh, Zhi-Quan Luo, and Sachin S Sapatnekar. A geometric programming-based worst case gate sizing method incorporating spatial correlation. IEEE transactions on computer-aided design of integrated circuits and systems, 27(2):295–308, 2008.
- Natasja Sluijk, Alexandre M Florio, Joris Kinable, Nico Dellaert, and Tom Van Woensel. A chance-constrained two-echelon vehicle routing problem with stochastic demands. Transportation Science, 57(1):252–272, 2023.

- A.Ihsan Sonmez, Adil Baykasoglu, Turkay Dereli, and I.Huseyin Filiz. Dynamic optimization of multipass milling operations via geometric programming. International Journal of Machine Tools and Manufacture, 39(2):297–320, 1999. ISSN 0890-6955. doi: [https://doi.org/10.1016/S0890-6955\(98\)00027-3](https://doi.org/10.1016/S0890-6955(98)00027-3). URL <https://www.sciencedirect.com/science/article/pii/S0890695598000273>.
- Mehran Spitmaan, Hyojung Seo, Daeyeol Lee, and Alireza Soltani. Multiple timescales of neural dynamics and integration of task-relevant signals across cortex. Proceedings of the National Academy of Sciences, 117(36):22522–22531, 2020.
- David Tank and J Hopfield. Simple ‘neural’ optimization networks: An a/d converter, signal decision circuit, and a linear programming circuit. IEEE transactions on circuits and systems, 33(5):533–541, 2003.
- Siham Tassouli and Abdel Lisser. A neural network approach to solve geometric programs with joint probabilistic constraints. Mathematics and Computers in Simulation, 205:765–777, 2023. ISSN 0378-4754. doi: <https://doi.org/10.1016/j.matcom.2022.10.025>. URL <https://www.sciencedirect.com/science/article/pii/S0378475422004384>.
- Stanislav Uryasev and Panos M Pardalos. Stochastic optimization: algorithms and applications, volume 54. Springer Science & Business Media, 2013.
- Oriol Vinyals, Alexander Toshev, Samy Bengio, and Dumitru Erhan. Show and tell: A neural image caption generator. In Proceedings of the IEEE conference on computer vision and pattern recognition, pages 3156–3164, 2015.
- Jun Wang. A deterministic annealing neural network for convex programming. Neural Networks, 7(4):629–641, 1994. ISSN 0893-6080. doi: [https://doi.org/10.1016/0893-6080\(94\)90041-8](https://doi.org/10.1016/0893-6080(94)90041-8). URL <https://www.sciencedirect.com/science/article/pii/0893608094900418>.
- Shuang Wang, Liping Pang, Hua Guo, and Hongwei Zhang. Distributionally robust optimization with multivariate second-order stochastic dominance constraints with applications in portfolio optimization. Optimization, 72(7):1839–1862, 2023.
- Wolfram Wiesemann, Daniel Kuhn, and Melvyn Sim. Distributionally robust convex optimization. Operations research, 62(6):1358–1376, 2014.
- Dawen Wu and Abdel Lisser. A deep learning approach for solving linear programming problems. Neurocomputing, 520:15–24, 2023.
- Tian Xia, Jia Liu, and Abdel Lisser. Distributionally robust chance constrained games under wasserstein ball. Operations Research Letters, 51(3):315–321, 2023a. ISSN 0167-6377. doi: <https://doi.org/10.1016/j.orl.2023.03.015>. URL <https://www.sciencedirect.com/science/article/pii/S0167637723000573>.
- Youshen Xia and Jun Wang. A recurrent neural network for nonlinear convex optimization subject to nonlinear inequality constraints. IEEE Transactions on Circuits and Systems I: Regular Papers, 51(7):1385–1394, 2004.
- Zicong Xia, Yang Liu, Jiasen Wang, and Jun Wang. Two-timescale recurrent neural networks for distributed minimax optimization. Neural Networks, 165:527–539, 2023b.
- Gongxian Xu and Lei Wang. An improved geometric programming approach for optimization of biochemical systems. Journal of Applied Mathematics, 2014(1):719496, 2014.
- Shu-Bo Yang and Zukui Li. Distributionally robust chance-constrained optimization with sinkhorn ambiguity set. AIChE Journal, 69(10):e18177, 2023.
- Alireza Zare, CY Chung, Junpeng Zhan, and Sherif Omar Faried. A distributionally robust chance-constrained milp model for multistage distribution system planning with uncertain renewables and loads. IEEE Transactions on Power Systems, 33(5):5248–5262, 2018.
- Maojun Zhang, Jiangxia Nan, and Gonglin Yuan. The geometric portfolio optimization with semivariance in financial engineering. Systems Engineering Procedia, 3:217–221, 2012. ISSN 2211-3819. doi: <https://doi.org/10.1016/j.sepro.2011.10.034>. URL <https://www.sciencedirect.com/science/article/pii/S2211381911001238>. Information Engineering and Complexity Science - Part I.
- Yiling Zhang, Siqian Shen, and S. Ayca Erdogan. Distributionally robust appointment scheduling with moment-based ambiguity set. Operations Research Letters, 45(2):139–144, 2017. ISSN 0167-6377. doi: <https://doi.org/10.1016/j.orl.2017.01.010>. URL <https://www.sciencedirect.com/science/article/pii/S0167637717300688>.
- Yue Zhao, Zhi Chen, and Zhenzhen Zhang. Distributionally robust chance-constrained p-hub center problem. INFORMS Journal on Computing, 35(6):1361–1382, 2023.